



HAL
open science

Accurate energy consumption for comparison of climate change impact of thermal and electric vehicles

Anatole Desreveaux, A. Bouscayrol, R. Trigui, E. Hittinger, E. Castex, G.M. Sirbu

► To cite this version:

Anatole Desreveaux, A. Bouscayrol, R. Trigui, E. Hittinger, E. Castex, et al.. Accurate energy consumption for comparison of climate change impact of thermal and electric vehicles. *Energy*, 2023, 268, pp.126637. 10.1016/j.energy.2023.126637 . hal-04251075

HAL Id: hal-04251075

<https://hal.science/hal-04251075>

Submitted on 20 Oct 2023

HAL is a multi-disciplinary open access archive for the deposit and dissemination of scientific research documents, whether they are published or not. The documents may come from teaching and research institutions in France or abroad, or from public or private research centers.

L'archive ouverte pluridisciplinaire **HAL**, est destinée au dépôt et à la diffusion de documents scientifiques de niveau recherche, publiés ou non, émanant des établissements d'enseignement et de recherche français ou étrangers, des laboratoires publics ou privés.

Accurate Energy Consumption for Comparison of Climate Change Impact of Thermal and Electric Vehicles

A. Desreuveaux¹, A. Bouscayrol¹, R. Trigui², E. Hittinger³, E. Castex⁴ and G. M. Sirbu⁵

¹ Univ. Lille, Arts et Metiers Institute of Technology, Centrale Lille, Junia, ULR 2697-L2EP, F-59000 Lille, France

² Univ Eiffel, Univ Lyon, ENTPE, LICIT-ECO7, F-69675 Lyon, France

³ Rochester Institute of Technology, Rochester, NY 14623, USA

³ Univ. Lille, ULR 4477 – TVES – Territoires Villes Environnement & Société, F- 59000, Lille, France

⁴ Renault Technologie Roumanie SRL, 062204, Bucharest, Romania

Abstract: Performing a climate impact assessment of vehicles is essential for comparing different powertrain options during an entire vehicle life. Life Cycle Assessment (LCA) is used to estimate these effects over a vehicle's lifecycle, including manufacturing, usage, and end-of-life phases. LCA comprises several indicators, such as the Global Warming Potential (GWP). Generally, LCA or GWP studies use manufacturer-reported standard cycle data to estimate the energy consumption of vehicles. In this article, we develop diesel, gasoline, and electric vehicle simulation tools using the Energetic Macroscopic Representation formalism to evaluate that practice. These simulations are validated with actual, measured driving cycles. The simulations are then used to compare the calculated GWP from real, measured driving cycles relative to standard driving cycles used as industry benchmarks. The results show that standard driving cycles consistently underestimate the benefit of switching from fossil fueled vehicles to electric vehicles. Finally, a sensitivity analysis of the battery life duration is included in this work. It shows that the replacement or second life of batteries is also a key parameter in the GWP advantages of electric vehicles.

Keywords: Electric vehicle, Conventional vehicle, Life cycle assessment, Global warming potential, Vehicle simulation

Highlights

- Global Warming Potential of European conventional and electric small cars are compared
- Benefits of EVs are larger in real driving cycles instead of standard ones
- Sensitivity analysis is done for EV battery life duration
- Battery second life increases the benefits of the electric vehicles up to 43%

1. Introduction

Electric Vehicles (EVs) are a promising solution to reduce greenhouse gas (GHG) emissions in the transportation sector [1]. Unfortunately, the production of the batteries that they require has a significant ecological impact [2]. For a fair comparison between thermal and electric vehicles, a Life Cycle Assessment (LCA) approach is needed. LCA enables the computation of several footprint indicators of a product [3][4]. The climate change indicator, also called Global Warming Potential (GWP), is related to GHG emissions during the entire lifecycle of the product, which is the focus of this paper. Several phases are considered in vehicle LCA. The manufacturing phase deals with the extraction of any materials, the manufacture of the complete vehicle and the related energy used in creating or delivering the product. The usage phase considers GHG from driving the vehicle, including the extraction of primary energy sources, conversion to the vehicle energy (e.g., gasoline or electricity), distribution of this energy and emissions when moving. The energy consumption of the vehicle is thus the key point for this phase. The end-of-life phase considers the GHGs due to recycling operations and waste management.

43 For a considered vehicle, the GHG of the manufacturing and end-of-life phases are constant as we consider a fixed number
44 of components (e.g., filters, tyres, etc.) changed during the life of the vehicle. Thus, the sizing of the battery is an essential
45 point of the EV assessment [5]. For EVs, battery replacement is an important concern [6]. When this occurs, the GHG
46 footprint of the vehicle is significantly increased. In addition, there is increasing research and development on the reuse
47 of the vehicle battery for a second life [7] [8]. In this case, the GHG footprint of battery production is shared with another
48 application. As the GHG of the battery is a significant contributor to the overall climate change indicator for EVs, a
49 sensitivity analysis of the battery life should be included in the LCA.

50 The usage phase GHG emissions strongly depend on the amount and type of travel realized by the vehicle. Moreover, for
51 EVs, the method of electricity production also has a strong impact [3]. When estimating the energy consumption of
52 electric vehicles, constant consumption factors are often used for modeling simplicity. Examples include 12.7
53 kWh/100km for a Volkswagen e-golf in Europe [6] or 20.6 kWh/100 km for a Nissan Leaf in Europe [9]. Other studies
54 use consumption factors from different manufacturers or regulatory entities within these limits [10]-[14]. These constant
55 factors are derived from standard driving cycles to compute the energy consumption of both thermal and electrical
56 vehicles [15][16]. Standard driving cycles are used throughout the vehicle development process, from the vehicle design
57 to its certification. Evaluation of a vehicle's energy consumption and pollutant emissions also uses these standard cycles.
58 There are numerous standard driving cycles that aim to represent the driving habits of different kinds of vehicles (e.g.,
59 cars, buses, etc.) and for different countries or regions [17][18].

60 But these driving cycles are not always representative of actual driving or energy use [19] and correction factors are
61 sometimes considered [20]. A recent study demonstrates that standard driving cycles underestimate the energy
62 consumption of thermal vehicles and overestimate those of EVs [21]. This suggests that most assessments of the
63 energy/carbon footprint of vehicle operations may be consistently biased in favor of thermal vehicles. A fair comparison
64 of GHG footprints of both types of vehicles requires realistic driving cycles. Some past work has focused on energy
65 consumption measured on the road [22][23]. This is logical and justifiable, but such results cannot be easily applied to
66 other vehicles and strongly depend on driving conditions (e.g., traffic) [24][25].

67 The objective of this paper is to provide a fair comparison of the GWP of three vehicles (diesel, gasoline and electric) by
68 using real measured driving cycles and to compare these results to traditional constant consumption factors. In Europe,
69 most vehicle sales at the beginning of the 2010s were diesel. However, in recent years, the diesel car market share has
70 fallen and has been progressively replaced by gasoline, while the EV market is rapidly developing [26]. **In this work,
71 three actual vehicles are considered, from the same small-car segment and the same manufacturer for a fair comparison.
72 The studied electric vehicle has been designed from the studied diesel vehicle which leads to an easier and more relevant
73 comparison. In the years up to 2020, the small car vehicle segment has been around 20% of the sales in the European
74 market [27]. Within that segment, 80% of the thermal cars have a 5-speed manual gearbox.**

75 An accurate simulation is developed to estimate the energy consumption of the three vehicles for any driving cycle. After
76 experimental validation of the simulation, real driving cycles are used as the input for later analysis. This method makes
77 it possible to have identical driving cycles in the different vehicles as well as a comparison with standardized test cycles.
78 The GWP of the different vehicles is then computed and the battery replacement or reuse is also considered. The diesel
79 and electric vehicle simulation has been developed for a prior economic comparison of both cars [21]. This simulation is
80 now extended to a gasoline car, and GWP indicators of the usage phase are implemented. Finally, the GWP of the three
81 life phases of the vehicles is computed to show the effect of improved resolution on usage phase energy use and emissions.

82 Section 2 presents the methodology. Section 3 develops the simulation of the vehicles and the validation by experimental
83 results. The Global Warming Potential of the different cars is compared in Section 4. Section 5 discusses the limitations
84 and advances of the proposed method.

85

86

87 2. Methodology

88 Three vehicles of the same segment are studied for a fair comparison: the Renault Clio (gasoline and diesel) and the
89 Renault Zoe (electric vehicle). An accurate simulation is then developed to estimate their GHG emissions in the usage
90 phase using real on-road driving cycles. Then their GWPs are computed for their entire life cycle.

91 2.1 Studied Vehicles

92 The chosen vehicles (Figure 1) are the Renault Zoé for the electric vehicle [28] and Renault Clio for thermal cars (i.e.,
93 diesel and gasoline) [29]. All three vehicles are in the small-car segment, also called B-segment in Europe. The EV has a
94 mass of 1480 kg including a Li-ion NMC battery of 41 kWh. The mass of the diesel and gasoline vehicles are respectively
95 1130 kg and 1080 kg. Due to the battery, the EV has a higher mass than the conventional ones.



96

97 Figure 1: Studied vehicles: Renault Zoé Q90 41 kWh 2016 and Renault Clio III 1.5 dci 90 hp -2015 (diesel car).

98 All three vehicles are composed of an energy source (the battery for the EV and the fuel tank for the thermal vehicles),
99 an energy transformer (electric motor for the EV and Internal Combustion Engine for the conventional cars), a gearbox,
100 wheels, mechanical brakes and a chassis. For the EV, the gearbox is composed of a simple gear connected to the
101 differential. **For model validation reasons, the gearbox is a 5-gear manual gearbox connected to the differential for the
102 thermal vehicles as used in most European vehicles. However, the method can be extended to newer gearbox technologies
103 when measurements are available. While the simulation of other gearbox designs is possible, the lack of on-road validation
104 of the simulation would limit the validity of the analysis in this work.**

105 2.2 Accurate energy consumption

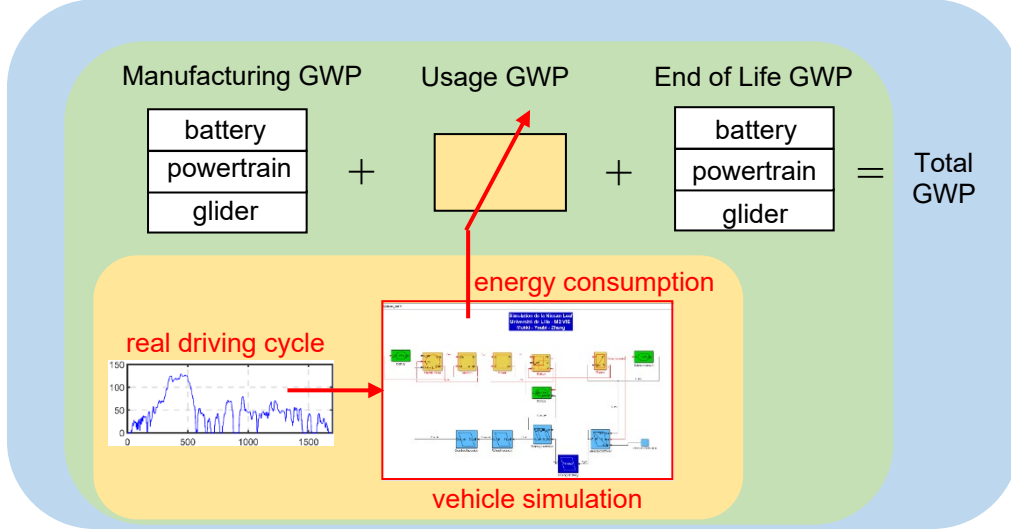
106 The general strategy in this research is first to develop accurate simulation models of each of the three vehicles, which
107 are validated with experimental testing. Next, the simulations can be used to compute the energy consumption of the three
108 vehicles using identical realistic driving cycles. There are several reasons for this strategy. First, it is impossible to have
109 precisely the same on-road driving conditions for each of the three vehicles. Even when traveling the same route with the
110 same driver, the traffic, weather, and streetlight conditions will vary. These differences lead to bias in comparisons of
111 energy consumption. Moreover, as the simulation is rapid, different driving cycles can be compared without the time and
112 cost needed to prepare the car (e.g., charging for the EV), drive, and recover the data.

113 The simulation is organized using Energetic Macroscopic Representation (EMR) [30]. EMR is a graphical formalism
114 used to organize the models of energy conversion systems and their controls. EMR has been widely used to study the
115 energy consumption of various electric and hybrid vehicles [31]-[33]. It enables a common framework for the simulation
116 of the studied electric, diesel and gasoline vehicles.

117 2.3 Computation of the Global Warming Potential

118 The vehicle GWP computation is decomposed into three phases (Figure 2). The manufacturing phase is related to 3
119 subsystems: the battery, the powertrain and the glider (i.e., the body and non-drive components). **The glider is assumed**

120 to be the same for all vehicles, as the Renault Zoe is built based on existing thermal vehicles, which is common for first-
 121 generation EVs. Indeed Renault Zoe has been designed as an electric version of the Renault Clio. The usage phase has
 122 the vehicle energy consumption as an input for a considered driving cycle. The energy consumption is computed from
 123 simulation combined with measured driving cycles, as explained above. For the end-of-life phase, the three initial
 124 subsystems are considered.



125
 126 Figure 2: Improved global warming potential computation with more accurate usage phase, through detailed simulation
 127 and real driving cycles.
 128

129 3. Energy consumption of the studied vehicles

130 3.1 Model of the electric vehicle

131 The EMR of the EV is presented from left to right (Figure 3). The battery is a green oval and describes the battery voltage
 132 u_{bat} as a function of the current i_{ed} and the Open Circuit Voltage (OCV), which depends on the battery State of Charge
 133 (SoC).
 134

$$135 \quad u_{bat} = OCV(SoC) - R_{bat}i_{bat} \quad (1)$$

136 The battery is connected to the electric drive, represented by a multi-physical element (orange circle). The drive is
 137 composed of an inverter and an electric motor. It transforms the electricity into mechanical energy on the rotating shaft
 138 of the motor. The drive equation gives the current i_{ed} as a function of u_{bat} , the motor torque T_m and the gearbox speed Ω_{wh} .

$$139 \quad i_{ed} = \frac{T_m \Omega_{gb}}{u_{bat}} \quad (2)$$

140 Next, the gearbox is represented by a mono-physical conversion element (orange square) which converts the motor torque
 141 T_m to the gearbox torque T_{gb} and the wheel speed Ω_{wh} to the gearbox speed Ω_{gb} through the gearbox ratio k_{gb} .

$$142 \quad \begin{cases} T_{gb} = k_{gb}T_m \\ \Omega_{gb} = k_{gb}\Omega_{wh} \end{cases} \quad (3)$$

143 The wheels are represented by an equivalent wheel with the radius R_{wh} , which converts the gearbox torque to the wheel
 144 force F_{wh} and the vehicle velocity v_v to the wheel speed (orange square).

$$145 \quad \begin{cases} F_{wh} = \frac{T_{gb}}{R_{wh}} \\ \Omega_{wh} = \frac{v_v}{R_{wh}} \end{cases} \quad (4)$$

146 The total force F_{tot} applied to the vehicle is the sum of the wheel force F_{wh} and the mechanical brake force F_{br} . This
 147 equation is represented by a coupling element (double orange squares).

$$148 \quad F_{tot} = F_{wh} + F_{br} \quad (5)$$

149 The chassis of the vehicle is an energy accumulation element (crossed orange rectangle) because its mass accumulates
 150 energy during accelerations and restores this energy during decelerations. In this element, the vehicle velocity v_v depends
 151 on the total force F_{tot} , the resistive force F_{res} and the mass of the vehicle M_v .

$$152 \quad v_v = \frac{1}{M_v} \int F_{tot} - F_{res} \quad (6)$$

153 This chassis is connected to the road (green oval). The resistive force is a function of the rolling resistance F_{roll} ,
 154 aerodynamic resistance F_{aero} and the slope resistance F_{slope} .

$$155 \quad F_{res} = F_{roll} + F_{aero} + F_{slope} \quad (7)$$

156 The inversion-based control of the vehicle is systematically deduced from the EMR. First, the accumulation element of
 157 the chassis is indirectly inverted using a control loop of the vehicle velocity (crossed light blue parallelogram). The total
 158 force reference F_{tot_ref} depends on the measured resistive force F_{res_mes} , a controller $C(x)$, a reference velocity v_{v_ref} which
 159 comes from the driving cycle profile and the measure of the vehicle velocity v_{v_mes} .

$$160 \quad F_{tot_ref} = F_{res_mes} + C((v_{v_ref} - v_{v_mes})) \quad (8)$$

161 The other EMR blocks are directly inverted. The inversion of the coupling element gives a distribution element (double
 162 light blue parallelogram) which splits the total force into the brake and wheel forces, F_{br_ref} and F_{wh_ref} , using a braking
 163 input k_{br} given by the braking strategy.

$$164 \quad \begin{cases} F_{wh_ref} = k_{br} F_{tot_ref} \\ F_{br_ref} = (1 - k_{br}) F_{tot_ref} \end{cases} \quad (9)$$

165 The inversion of the wheel is the direct inversion of equation (4):

$$166 \quad T_{gb_ref} = R_{wh} F_{wh_ref} \quad (10)$$

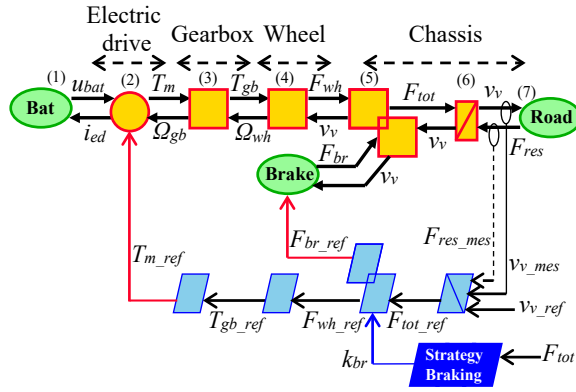
167 The reference torque applied to the motor T_{m_ref} depends on the gearbox reference torque and the gearbox ratio.

$$168 \quad T_{m_ref} = \frac{T_{gb_ref}}{k_{gb}} \quad (11)$$

169 Finally, the braking strategy distributes the forces between the wheel and the brakes (dark blue parallelogram). As the
 170 electric motor is reversible, energy can be recovered during braking phases in an EV. The energy recovery depends on
 171 several constraints, such as the maximal battery current and SoC. When the vehicle is in the braking phase, the total force
 172 applied to the car is negative. In this configuration, the braking coefficient k_{br} is set to 60 % and can be limited if the
 173 battery current reaches its charging limitation or the battery is full (SoC >99 %). When the vehicle is not in the braking
 174 phase, the braking coefficient is set to 1.

$$175 \quad \begin{cases} k_{br} = 0.6 \text{ when } F_{tot_ref} < 0 \\ k_{br} = 1 \text{ when } F_{tot_ref} \geq 0 \end{cases} \quad (12)$$

176



177

178 Figure 3: EMR of the electric vehicle

179

180 **3.2 Model of the thermal vehicles**

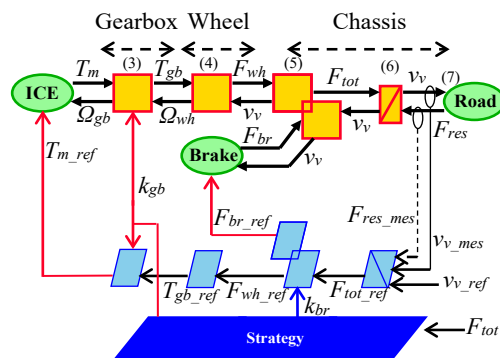
181 The EMR of the thermal vehicles is represented in figure 4. The two cars have the same representation. The only difference
 182 is the fuel used by the vehicles. The Internal Combustion Engine (ICE) is the energy source of the thermal vehicles (left
 183 green oval). The consumption of diesel and gasoline vehicles is calculated using a consumption map for each car. These
 184 maps are a function of the motor torque and speed. It is assumed an ideal control of the ICE:

185
$$T_{ice} = T_{ice_ref} \tag{10}$$

186 The ICE is connected to the manual gearbox of the vehicle (orange square). The equation of the gearbox is the same as
 187 the EV (3). In this vehicle, the gearbox ratio can take five different values. These values are selected in the strategy as a
 188 function of the vehicle velocity.

189 The manual gearbox is connected to the wheels (orange square). The wheel equation is given by (4). The wheel is coupled
 190 with the brakes (double orange squares) (5) and the chassis of the vehicle (crossed orange rectangle) (6). The chassis is
 191 connected to the road (right green oval) (7).

192 The control of the vehicle is deduced (light blue parts) directly from the EMR of the vehicle. In these cars, the brakes are
 193 only mechanical. So, when the total force F_{tot_ref} is positive, the wheel force F_{wh_ref} is equal to the total force F_{tot_ref}
 194 and the brake force F_{br_ref} is equal to 0. And when the total power is negative, the wheel force is null and the brake force is
 195 similar to the total force.



196

197 Figure 4: EMR of the thermal vehicles

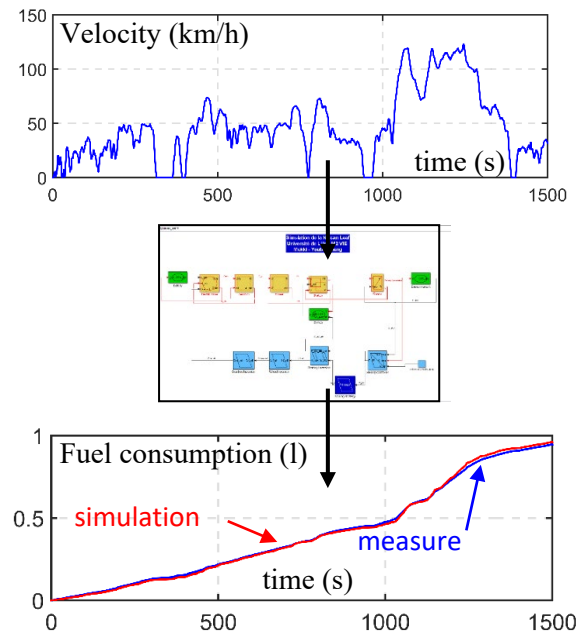
198

199 **3.3 Validation of the diesel vehicle**

200 After the achievement of the simulation tools of the vehicles above, they are validated by comparison with real
201 measurements from the cars during on-road driving. For each car, the velocity is measured with a GPS (Global Positioning
202 System) device and the energy consumption is read on the Can Bus of the cars through an OBD (On-Board Diagnostic)
203 reader. In this article, only the validation for the diesel vehicle is presented. The validation of the electric vehicle is similar
204 and detailed in [34].

205 The velocity profile is introduced in the simulation tool and the consumption is calculated for each test and compared
206 with the measured consumption (Fig. 5). For the real trip, the measured fuel consumption is 4.88 l/100 km. The fuel
207 consumption calculated by the simulation is 4.91 l/100 km. That leads to an error of about 1%.

208



209

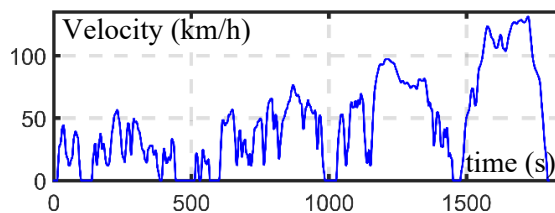
210 Figure 5: Validation approach of the diesel vehicle

211 After the validation of the different vehicle simulation tools, they can be used to calculate the energy consumption and
212 then the GHG emissions for each vehicle for different driving cycles.

213

214 **3.4 Comparison of the energy consumption using a standard driving cycle (WLTC)**

215 In this part, the simulation results and the data from the manufacturers are compared on the basis of the energy
216 consumption of the vehicles and the GWP in the usage phase, also called Well-to-Wheel emissions. The standard driving
217 cycle is the World Light vehicles Test Cycle (WLTC) class 3, adopted in Europe in 2017 (Fig. 6). This driving cycle is
218 now the standard used to estimate the pollutant emissions and energy consumption of the vehicles on roads in Europe.



219

220 Figure 6: Velocity of the WLTC driving cycle

221 The WLTC driving cycle is used with the vehicle simulations developed above and compared to manufacturer-reported
 222 energy efficiency (Table 1). The fuel efficiency data are referred to as “reported values” in the remainder of this article.
 223 For the thermal vehicles, the data are taken from [35]. Notably, this method suggests that the reported fuel consumption
 224 is underestimated by about 10 %. Using the reported value, which is commonly done in studies of vehicle GWP, would
 225 reduce the calculated climate impact of conventional thermal vehicles. For the EV, the reported value is taken from [35]
 226 and [36]. It appears to overestimate the consumption of the vehicle by about 17%. Thus, the energy and GWP of the EV
 227 may be regularly overestimated when using the reported values for energy efficiency. These calculations imply that the
 228 GWP of these vehicles may be consistently misestimated in favor of thermal vehicles, affecting a wide variety of
 229 conclusions and vehicle regulation decisions. It also highlights the importance of accurate energy consumption inputs for
 230 improved accuracy in GWP studies. Right now, standard driving cycles are generally used even if they are not
 231 representative [19].

232 Table 1: Evaluation of the consumption and emission due to the WLTC driving cycles for the different vehicles

Vehicles	Gasoline Vehicle	Diesel Vehicle	Electric Vehicle
Simulated energy consumption	4.8 L/ 100km	4.6 L/ 100km	17.1 kWh/ 100km
Reported energy consumption	4.3 L/ 100km	4.1 L/ 100km	20.1 kWh/ 100km

233

234 4. Global warming potential of the different vehicles

235 In this section, the inventory of the GWP for the manufacturing and end-of-life phases of the vehicles is integrated with
 236 the impact of the use phase, estimated with varying driving cycles. Finally, the effect of battery second life is discussed.

237 4.1 Global warming potential inventory of the studied vehicles

238 While the manufacturing and end-of-life phases of the vehicle lifecycle are not the focus of this work, they are included
 239 in order to show how usage phase misestimation affects overall GWP. The GWP inventory of the manufacturing and end-
 240 of-life of the various vehicle components is given in Tables 2 and 3. All vehicles use the same glider, as the studied
 241 electric vehicle design is derived from the conventional ones. The inventory of conventional vehicles is based on [37]. A
 242 reduction coefficient of 0.83 is applied to convert from a medium-size vehicle into a small-size vehicle. This coefficient
 243 is based on the methodology used to study different vehicle segments [5]. The Electric Vehicle inventory comes from
 244 prior work during the PANDA project [34], including a detailed GWP estimation of the battery.

245 The 41 kWh NMC battery of the electric car is a Lithium Ion battery with a Nickel Manganese Cobalt anode and a graphite
 246 cathode. All battery parts are produced in Asia and assembled in France. As the battery’s end-of-life is uncertain, it is
 247 assumed that the battery has been split into several parts which are disposed, recycled or re-purposed. Recycling has been
 248 realized by hydrometallurgical processes. The glider and powertrains of the vehicles are produced in Europe. The final
 249 assembly and dismantling of the vehicle are also realized in Europe.

250 Table 2: GWP inventory of the manufacturing of the studied vehicles (kg CO₂eq)

Components	Gasoline Vehicle	Diesel Vehicle	Electric Vehicle
Battery	0	0	4650
Powertrain	591	661	356
Glider	3900	3900	3900

251

252 Table 3: GWP inventory of the end-of-life of the studied vehicles (kg CO₂eq)

Components	Gasoline Vehicle	Diesel Vehicle	Electric Vehicle
Battery	0	0	634
Powertrain	41	46	25
Glider	271	271	271

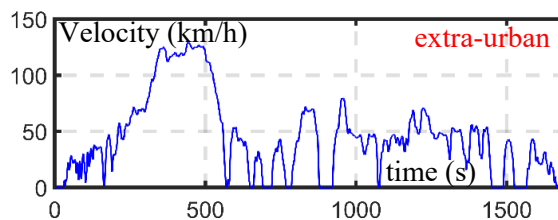
253

254

255 The considered electricity mix is 449 g CO₂eq/kWh. This value is based on the average European electricity mix and
 256 includes charging and distribution losses [34]. The GHG emissions of fuel production and usage are based on the average
 257 value given by the Joint Research Center of the European Commission [38]. These GHG emissions include emissions
 258 from the three most important gases emitted by fuel combustion: CO₂, CO, CH₄ and NO₂. The lifetime mileage for the
 259 different vehicles is set to 150 000 km, a typical value used in such studies [3]. The initial assumption for battery life is
 260 that the battery could be used for this distance and its life cycle is ended with the end of life of the vehicle. This assumption
 261 is investigated further at the end of this paper.

262 **4.2 Global Warming Potential of the studied vehicles on extra-urban driving cycles**

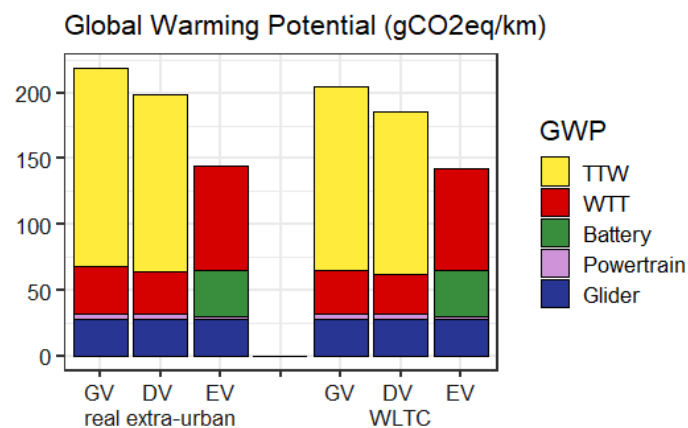
263 The global warming potential of the three vehicles is detailed for a real, measured extra-urban driving cycle (Figure 7).
 264 **These cycles have been selected to be representative of real trips realized in Europe.** The GWP of the usage phase is
 265 computed from the simulations of the three cars. For all vehicles, the usage phase is decomposed into two parts: the
 266 emission during the driving phase (also called tank-to-wheel, TTW) and the emissions due to the production of the energy
 267 (also called well-to-tank, WTT). The simulation of the different vehicles leads to an emission of 36 g CO₂eq/ km, 32 g
 268 CO₂eq/km and 79 g CO₂eq/km for the well-to-tank of the gasoline, diesel and electric vehicles. For the tank-to-wheel, the
 269 real extra-urban driving cycle leads to the emission of 187 g CO₂eq/km and 156 g CO₂eq/km for gasoline and diesel cars.
 270 Of course, there is no direct CO₂ emission from EVs during driving.



271
 272 Figure 7: Real extra-urban driving cycle

273 The total GWP can thus be computed, including all phases. The EV has a climate impact of 140 gCO₂eq/km. The diesel
 274 has an impact of 198 gCO₂eq/km and the gasoline vehicle is 219 gCO₂eq/km. As expected, the electric car has the lowest
 275 use phase GWP of the three vehicles despite the relatively high impact of the battery manufacturing and end-of-life.

276 **The GWP is also computed for the WLTC, the standard extra-urban driving cycle used in Europe. Between 2017 and**
 277 **2021, automaker figures are estimated using a WLTC driving cycle and calculated for the NEDC cycle (which was the**
 278 **standard cycle until 2017) using a corrective factor.** However, we prefer to compute them by simulation to ensure that all
 279 calculations use the same process, which leads to similar figures as those reported by automakers. A lifecycle GWP
 280 comparison is then carried out for the three vehicles (Fig. 8). For all vehicles, the estimated GWP is reduced by using the
 281 WLTC instead of the real extra-urban driving cycles by 7% for the two conventional vehicles and 1% for the electric
 282 vehicle. Thus, once again, the standard driving cycles favor the thermal vehicles in comparison with the real driving
 283 cycles.



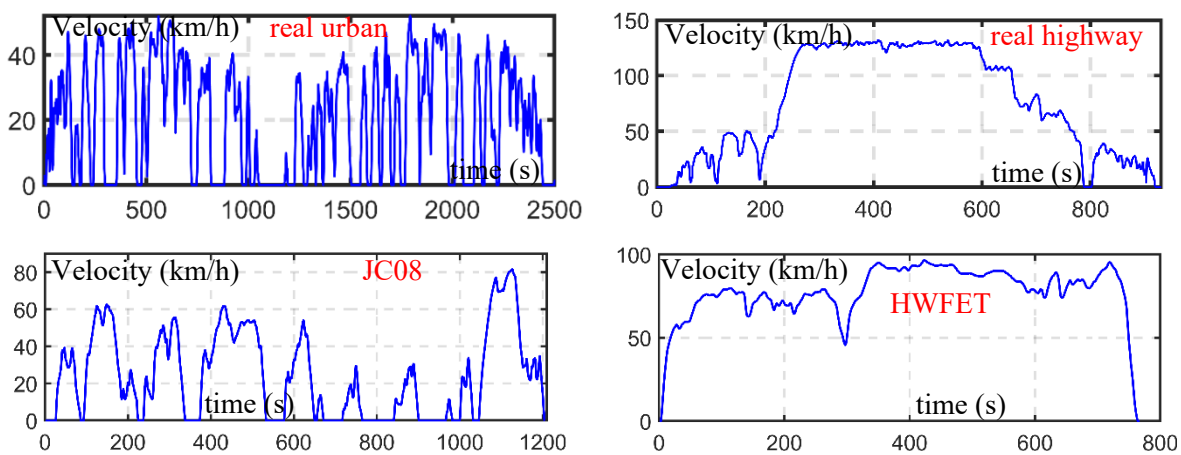
284

285 Figure 8: GWP of the gasoline (GV), diesel (DV) and electric (EV) vehicles for a real extra-urban driving cycle and
 286 WLTC.

287 It has been demonstrated that the NEDC leads to lower estimates of energy consumption and pollutant emission than the
 288 WLTC for the usage phase [19]. As some studies still use NEDC as a driving cycle, the benefits of transitioning from
 289 conventional to electric vehicles would be further underestimated in terms of GWP.

290 4.3 Impact of different driving cycles on the Global Warming Potential

291 In order to demonstrate that the effects described above are consistent, this section compares the GWP from different
 292 driving cycles, between gasoline and electric vehicles. The gasoline vehicle is selected because it is the highest CO₂
 293 emitter. The results of the diesel vehicle will thus be between the gasoline and electric vehicles. We introduce two
 294 additional real, measured driving cycles. **These driving cycles represent urban and highway road conditions which can be**
 295 **found in Europe.** We compare them with equivalent standard driving cycles (Figure 9). The two upper driving cycles are
 296 real ones measured with the electric vehicle. The two bottom driving cycles are the JC08, the Japanese standard driving
 297 cycle and the HWFET, an American highway standard driving cycle.



298
 299 Figure 9: Four additional driving cycles used in this analysis

300 For each velocity profile, the Global Warming Potential of the usage phase is calculated using the vehicle simulation tools
 301 (Table 4).

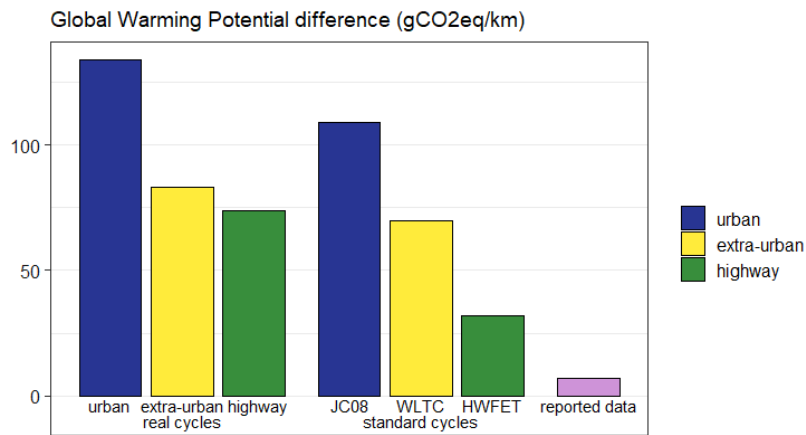
302 Table 4: GWP for the gasoline and electric vehicles for the different cycles (g CO₂eq/km)

Driving cycles	Real urban	JC08	Real highway	HWFET
Gasoline Vehicle	223	191	202	125
Electric Vehicle	64	57	103	68

303
 304 The difference in the GWP between gasoline and electric vehicles (g CO₂eq/km for the gasoline vehicle minus g
 305 CO₂eq/km for the electric vehicle) for the six considered driving cycles is presented in Figure 10. The GWP difference is
 306 about 83 g CO₂eq/km for the extra-urban driving cycle, with higher emissions per km for urban driving and lower
 307 emissions per km on highways. In all cases, the EV has a lower climate impact per km, but the advantage of EVs is
 308 consistently underestimated when standard driving cycles are used. Relative to the real extra-urban driving cycle, using
 309 the standard WLTC driving cycle reduces the benefits of switching to EV by 16% (from 83 g CO₂eq/km to 70 g
 310 CO₂eq/km). For the JC08 driving cycle, the benefits of switching to EV are reduced by 23% (from 134 g CO₂eq/km to
 311 109 g CO₂eq/km) relative to the real urban driving cycle. And for highways, the standard HWFET cycle underestimates
 312 the emissions advantage of EVs by 57% (from 74 g CO₂eq/km to 32 g CO₂eq/km). Moreover, the GWP for the two
 313 vehicles has also been calculated from the reported consumption data given in Table 1. The GWP difference, in this case,
 314 is 7 g CO₂eq/km. Once again, these comparisons show the importance of considering real driving cycles when estimating
 315 GWP potential of vehicles instead of the common practice in the literature of using manufacturers' reported data. As

316 explained above, the difference between the diesel and electric vehicle are lower as the gasoline vehicle has more GWP
 317 in the usage phase than the diesel vehicle.

318



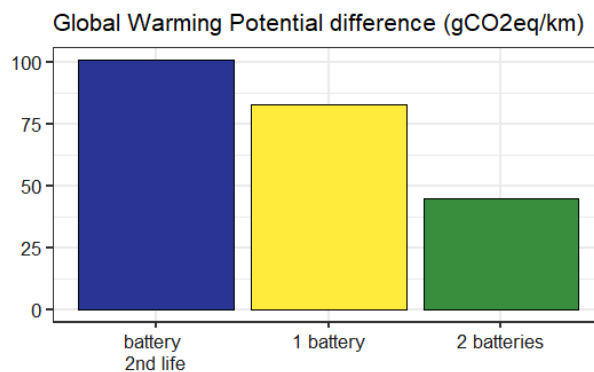
319

320 Figure 10: GWP difference between the gasoline and electric vehicles as a function of the driving cycle

321 **4.4 Impact of the battery lifetime and second life**

322 We have also investigated the effect of the battery usage/replacement on the difference in climate change impact between
 323 gasoline and electric vehicles, using the real extra-urban driving cycle (Fig. 11). In the results above, the battery is
 324 assumed to be at the end of its life at the same time as the end of the vehicle's life. This case corresponds to a GWP
 325 difference of 83 g CO₂eq/km between gasoline and electric vehicles. Two other scenarios are considered for the battery
 326 life duration. First, a second life of the battery is assumed, for example in a stationary application [8]. The GWP of the
 327 battery is thus split between the vehicle use and the secondary use. For simplification, an equivalent usage time is
 328 considered for the vehicle and the secondary services (i.e., a coefficient of 0.5 is applied to the battery manufacturing and
 329 end-of-life contribution). In this case, the GWP benefit of the EV is increased by 22% (from 83 g CO₂eq/km to 101 g
 330 CO₂eq/km). Second, we consider a case where two batteries are required during the vehicle's lifetime. This case
 331 corresponds to rapid aging during the usage phase (e.g. frequent ultra-fast charging). In this second case, the GWP benefit
 332 of an EV is reduced by 43% (from 83 g CO₂eq/km to 45 g CO₂eq/km). Once again, the difference between the diesel and
 333 electric vehicles are lower as the gasoline vehicle has the largest GWP in the usage phase.

334



335

336 Figure 11: GWP difference between gasoline and electric vehicles as a function of the battery usage for the real extra-
 337 urban driving cycle

338

339

340

341 5. Conclusion

342 This work offers a comparison of climate change impacts of different driving cycles for conventional and electric vehicles
343 in Europe. In order to have accurate values of the GHG emissions during the usage phase, vehicle simulation tools have
344 been developed and connected to GWP studies. These simulation tools were validated by comparison with measurements
345 from real vehicles and used to illustrate the systematic biases of traditional standard driving cycles.

346 We applied the same driving cycles for each vehicle in order to have a fair comparison of the climate effects of vehicle
347 operation. However, the experimental basis of this work means that it is limited in scope. The driving cycles in this study
348 do not cover all possible trips and driving conditions such as traffic, driving behavior, or weather conditions. In addition,
349 this work proposes only one comparison between two B-segment vehicles with manual gearboxes which are the main
350 mechanical transmissions in conventional vehicles. Further experimentation and analysis are necessary to explore all the
351 options available on the market: other segments (sedan, SUV), other propulsion (hybrids) or different gearboxes
352 (automated, Dual clutch Transmission). However, we propose that the results above give sufficient information to have
353 fair comparisons between the studied vehicles and to illustrate an important bias in existing studies.

354 The results show a lower GWP for EVs, relative to thermal vehicles, in the case of the current European electricity mix.
355 Furthermore, this work highlights the importance of considering real driving cycles instead of relying on traditional
356 standard cycles and the manufacturer-reported data that comes from data sheets. Standard driving cycles underestimate
357 the benefits of EVs in terms of GWP. As EVs are more commonly used on urban roads, we consider that real driving
358 cycles are more representative for the EV. In this case, standard driving cycles reduce the potential GWP benefits of EVs
359 by 50% relative to real urban driving cycles. Consequently, the scope of GWP or LCA studies should mention the type
360 of driving cycles used and consider which driving assumptions are most appropriate.

361 Finally, the analysis of battery life opens further discussions. The analysis in this paper focuses on the NMC battery which
362 represents around 80 % of the batteries present in vehicles [1]. The consideration of the secondary use of the battery leads
363 to a reduction of the GWP of the EV. Such a practice would further increase the benefits of EVs in terms of GWP. This
364 discussion can be improved with better knowledge and data about the lifetime of a battery for an electric vehicle in both
365 vehicle usage and secondary life usage. Battery technology also has an important GWP impact due to both recycling and
366 reuse [39][40]. Other chemistries used in EVs, like LFP which has a longer lifetime than NMC [41], can be studied in the
367 future.

368 This work only considers electric and thermal vehicles. Hybrid vehicles such as hybrids electric vehicles and fuel cell
369 electric vehicles are not considered. For these vehicles, intermediary results on the GWP can be expected [5]. However,
370 these kinds of vehicles can have different designs (series, parallel) and different levels of hybridization (micro to full
371 hybrid) [42]. Furthermore, energy management and the driving cycle also have an impact on GWP potential [43]. Due to
372 the high number of parameters, it is much more complex to give accurate figures for these vehicles.

373 This work does not include a detailed analysis of the manufacturing and end-of-life phases of the vehicles. In fact, the
374 manufacturing of the engine of conventional vehicles is more complex over time and the use of resources is more relevant.
375 For EVs, battery sizes are still increasing and the battery recycling processes are still mostly unknown. While these details
376 are being investigated by other researchers, these limitations have an impact on the results. These gaps will be studied in
377 future work.

378 6. Acknowledgment 379

380 This paper has been achieved within the framework of the PANDA project, which has received funding from the European
381 Union's Horizon 2020 research and innovation program under grant agreement no. 824256 (PANDA). The work has also
382 been performed within the CUMIN program (e-mobility campus of the University of Lille) and MEGEVH (French
383 network on electrified vehicles).

384

385 7. References

- 386
387 [1] “Global EV outlook 2022, “Securing supplies for an electric future”, International Energy Agency report, 2022.
388 [2] J. F. Peters, M. Baumann, B. Zimmermann, J. Braun, et M. Weil, « The environmental impact of Li-Ion batteries and
389 the role of key parameters – A review », *Renewable and Sustainable Energy Reviews*, vol. 67, p. 491-506, janv. 2017,
390 doi: [10.1016/j.rser.2016.08.039](https://doi.org/10.1016/j.rser.2016.08.039)
391 [3] B. Marmiroli, M. Messagie, G. Dotelli, J. Van Mierlo, « Electricity Generation in LCA of Electric Vehicles: A
392 Review”, *Applied Sciences*, vol. 8, n°8: 1384, 2018, doi: 10.3390/app8081384.
393 [4] K. J. Dillman, A. Árnadóttir, J. Heinonen, M; Czekiewicz, B. Davíðsdóttir, “Review and Meta-Analysis of EVs:
394 Embodied Emissions and Environmental Breakeven”, *Sustainability*, vol°12,n° 22, 9390 ,2020, doi:
395 10.3390/su12229390
396 [5] B. Cox, C. Bauer, A. Mendoza Beltran, D. P. Van Vuuren, C. L. Mutel, « Life cycle environmental and cost
397 comparison of current and future passenger cars under different energy scenarios” *Applied Energy*, vol. 269, P.
398 115021, 2020, doi: 10.1016/j.apenergy.2020.115021.
399 [6] R. Kawamoto, H. Mochizuki, Y. Moriguchi, T. Nakano, M. Motohashi, Y. Sakai, A. Inaba , « Estimation of CO2
400 Emissions of Internal Combustion Engine Vehicle and Battery Electric Vehicle Using LCA », *Sustainability*, vol. 11,
401 n° 9, Art. n° 9, janv. 2019, doi: [10.3390/su11092690](https://doi.org/10.3390/su11092690).
402 [7] C. S. Ioakimidis, A. Murillo-Marrodán, A. Bagheri, D. Thomas, et K. N. Genikomsakis, « Life Cycle Assessment of
403 a Lithium Iron Phosphate (LFP) Electric Vehicle Battery in Second Life Application Scenarios », *Sustainability*, vol.
404 11, n° 9, n° 9, janv. 2019, doi: [10.3390/su11092527](https://doi.org/10.3390/su11092527).
405 [8] E. Hossain, D. Murtaugh, J. Mody, H. M. R. Faruque, M. S. Haque Sunny and N. Mohammad, "A Comprehensive
406 Review on Second-Life Batteries: Current State, Manufacturing Considerations, Applications, Impacts, Barriers &
407 Potential Solutions, Business Strategies, and Policies," *IEEE Access*, vol. 7, pp. 73215-73252, 2019, doi:
408 10.1109/ACCESS.2019.2917859.
409 [9] K. Petrauskienė, M. Skvarnavičiūtė, et J. Dvarionienė, « Comparative environmental life cycle assessment of electric
410 and conventional vehicles in Lithuania », *Journal of Cleaner Production*, vol. 246, p. 119042, févr. 2020, doi:
411 [10.1016/j.jclepro.2019.119042](https://doi.org/10.1016/j.jclepro.2019.119042).
412 [10] Ö. Andersson et P. Börjesson, « The greenhouse gas emissions of an electrified vehicle combined with renewable
413 fuels: Life cycle assessment and policy implications », *Applied Energy*, vol. 289, p. 116621, mai 2021, doi:
414 [10.1016/j.apenergy.2021.116621](https://doi.org/10.1016/j.apenergy.2021.116621).
415 [11] K. Bekel et S. Pauliuk, « Prospective cost and environmental impact assessment of battery and fuel cell electric
416 vehicles in Germany », *Int J Life Cycle Assess*, vol. 24, n° 12, p. 2220-2237, déc. 2019, doi: [10.1007/s11367-019-](https://doi.org/10.1007/s11367-019-01640-8)
417 [01640-8](https://doi.org/10.1007/s11367-019-01640-8).
418 [12] Q. Qiao, F. Zhao, Z. Liu, X. He, et H. Hao, « Life cycle greenhouse gas emissions of Electric Vehicles in China:
419 Combining the vehicle cycle and fuel cycle », *Energy*, vol. 177, p. 222-233, juin 2019, doi:
420 [10.1016/j.energy.2019.04.080](https://doi.org/10.1016/j.energy.2019.04.080).
421 [13] Z. Yang, B. Wang, et K. Jiao, « Life cycle assessment of fuel cell, electric and internal combustion engine vehicles
422 under different fuel scenarios and driving mileages in China », *Energy*, vol. 198, p. 117365, mai 2020, doi:
423 [10.1016/j.energy.2020.117365](https://doi.org/10.1016/j.energy.2020.117365).
424 [14] M. Kannangara, F. Bensebaa, et M. Vasudev, « An adaptable life cycle greenhouse gas emissions assessment
425 framework for electric, hybrid, fuel cell and conventional vehicles: Effect of electricity mix, mileage, battery capacity
426 and battery chemistry in the context of Canada », *Journal of Cleaner Production*, vol. 317, p. 128394, oct. 2021, doi:
427 [10.1016/j.jclepro.2021.128394](https://doi.org/10.1016/j.jclepro.2021.128394).
428 [15] S. Xiong, Y. Wang, B. Bai, et X. Ma, « A hybrid life cycle assessment of the large-scale application of electric
429 vehicles », *Energy*, vol. 216, p. 119314, févr. 2021, doi: [10.1016/j.energy.2020.119314](https://doi.org/10.1016/j.energy.2020.119314).
430 [16] H. Ambrose, A. Kendall, M. Lozano, S. Wachche, et L. Fulton, « Trends in life cycle greenhouse gas emissions of
431 future light duty electric vehicles », *Transportation Research Part D: Transport and Environment*, vol. 81, p. 102287,
432 avr. 2020, doi: [10.1016/j.trd.2020.102287](https://doi.org/10.1016/j.trd.2020.102287).
433 [17] M. André, « The ARTEMIS European driving cycles for measuring car pollutant emissions », *Science of The Total
434 Environment*, vol. 334-335, p. 73-84, déc. 2004, doi: [10.1016/j.scitotenv.2004.04.070](https://doi.org/10.1016/j.scitotenv.2004.04.070).
435 [18] T.J. Barlow, S. Latham, I.S. McCrae, P. G. Boulter, *A reference book of driving cycles for use in the measurements
436 of road vehicle emissions*, TRL published report, 2009, ISBN 978-18-46-08816-2
437 [19] G. Fontaras, N. G. Zacharof, B. Ciuffo, “Fuel consumption and CO2 emissions from passenger cars in Europe –
438 Laboratory versus real-world emissions” *Progress in Energy and Combustion Science*, vol. 60, pp. 97–131, 2017
439 [20] C. Tagliaferri, S. Evangelisti, F. Acconcia, T. Domenech, P. Ekins, D. Barletta, P. Lettieri, “Life cycle assessment of
440 future electric and hybrid vehicles: A cradle-to-grave systems engineering approach “, *Chem. Eng. Res. and Design*,
441 vol. 112, pp. 298-309, 2016, doi: 10.1016/j.cherd.2016.07.003
442 [21] A. Desreveaux, E. Hittinger, A. Bouscayrol, E. Castex and G. M. Sirbu, "Techno-Economic Comparison of Total
443 Cost of Ownership of Electric and Diesel Vehicles," *IEEE Access*, vol. 8, pp. 195752-195762, 2020, doi:
444 10.1109/ACCESS.2020.3033500.
445 [22] M. Held et M. Schücking, « Utilization effects on battery electric vehicle life-cycle assessment: A case-driven
446 analysis of two commercial mobility applications », *Transportation Research Part D: Transport and Environment*,
447 vol. 75, p. 87-105, oct. 2019, doi: [10.1016/j.trd.2019.08.005](https://doi.org/10.1016/j.trd.2019.08.005).
448 [23] P. Marques, R. Garcia, L. Kulay, et F. Freire, « Comparative life cycle assessment of lithium-ion batteries for electric
449 vehicles addressing capacity fade », *Journal of Cleaner Production*, vol. 229, p. 787-794, août 2019, doi:
450 [10.1016/j.jclepro.2019.05.026](https://doi.org/10.1016/j.jclepro.2019.05.026).
451 [24] H. Achour and A. G. Olabi, “Driving cycle developments and their impacts
452 on energy consumption of transportation,” *Journal of Cleaner Production*, vol. 112, pp. 1778–1788, Jan. 2016.
453 [25] E. Ericsson, “Variability in urban driving patterns,” *Transportation Research Part D*, vol. 5,
454 pp. 337–354, 2000

- 455 [26] S. Diaz, P. Mock, Y. Bernard, G. Bieker, I. Pniewska, P.-L. Ragon, F. Rodriguez, U. Tietge, S. Wappelhorst,
 456 "European Vehicle Market Statistics, Pocketbook 2020-2021", International Council of Clean Transportation (ICCT)
 457 report, Editor: International Council of Clean Transportation Europe
- 458 [27] Vehicle market share by segment in the first half of 2022 [Online] Available: [https://www.jato.com/h1-2022-europe-](https://www.jato.com/h1-2022-europe-by-segments/)
 459 [by-segments/](https://www.jato.com/h1-2022-europe-by-segments/), accessed on 2022-12-07
- 460 [28] Renault Zoe [Online] Available: <http://www.renault.fr/vehicules/vehicules-electriques/zoe>, accessed on 2022-08-26.
- 461 [29] Renault Clio [Online] Available: <https://www.renault.fr/vehicules/particuliers/cliio.html>, accessed on 2022-08-26.
- 462 [30] A. Bouscayrol, J. P. Hautier, B. Lemaire-Semail, "Graphic Formalisms for the Control of Multi-Physical Energetic
 463 Systems", Systemic Design Methodologies for Electrical Energy, tome 1, Analysis, Synthesis and Management,
 464 Chapter 3, ISTE Willey editions, October 2012, ISBN: 9781848213883.
- 465 [31] K. Chen, A. Bouscayrol, A. Berthon, P. Delarue, D. Hissel, and R. Trigui, "Global modeling of different vehicles,"
 466 *IEEE Veh. Technol. Mag.*, vol. 4, no. 2, pp. 80–89, 2009. doi: 10.1109/MVT.2009.932540
- 467 [32] A. Castaings, W. Lhomme, R. Trigui, et A. Bouscayrol, « Comparison of energy management strategies of a
 468 battery/supercapacitors system for electric vehicle under real-time constraints », *Applied Energy*, vol. 163, p.
 469 190-200, 2016, doi: [10.1016/j.apenergy.2015.11.020](https://doi.org/10.1016/j.apenergy.2015.11.020).
- 470 [33] L. Horrein, A. Bouscayrol, Y. Cheng, C. Dumand, G. Colin, et Y. Chamailard, « Influence of the heating system on
 471 the fuel consumption of a hybrid electric vehicle », *Energy Conversion and Management*, vol. 129, p. 250-261, 2016,
 472 doi: [10.1016/j.enconman.2016.10.030](https://doi.org/10.1016/j.enconman.2016.10.030).
- 473 [34] G. M. Sirbu, A. Desrevelaux, C. Husar, N. Boicea, « Report of the virtual testing of the BEV », PANDA H2020 project
 474 report, January 2021, [Online] Available: <https://project-panda.eu/> accessed on 2022-09-01
- 475 [35] M. Scorrano, R. Danielis and M. Giansoldati, "Dissecting the total cost of ownership of fully electric cars in Italy:
 476 The impact of annual distance travelled home charging and urban driving", *Res. Transp. Econ.*, vol. 80, May 2020.
- 477 [36] M. Vilaça, G. Santos, M. S. A. Oliveira, M. C. Coelho, et G. H. A. Correia, « Life cycle assessment of shared and
 478 private use of automated and electric vehicles on interurban mobility », *Applied Energy*, vol. 310, p. 118589, mars
 479 2022, doi: [10.1016/j.apenergy.2022.118589](https://doi.org/10.1016/j.apenergy.2022.118589).
- 480 [37] C. Bauer, J. Hofer, H.-J. Althaus, A. Del Duce, A. Simons, "The environmental performance of current and future
 481 passenger vehicles: Life cycle assessment based on a novel scenario analysis framework", *Applied Energy*, vol. 157,
 482 pp. 871-883, 2015 doi: 10.1016/j.apenergy.2015.01.019.
- 483 [38] M. Prussi, M. Yugo, L. De Prada, M. Padella, R. Edwards. JEC Well-To-Wheels report v5. EUR 30284 EN,
 484 Publications Office of the European Union, Luxembourg, 2020, ISBN 978-92-76-20109-0, doi: 10.2760/100379,
 485 JRC121213.
- 486 [39] R. E. Ciez et J. F. Whitacre, « Examining different recycling processes for lithium-ion batteries », *Nat Sustain*, vol.
 487 2, n° 2, Art. n° 2, févr. 2019, doi: [10.1038/s41893-019-0222-5](https://doi.org/10.1038/s41893-019-0222-5).
- 488 [40] J. Zhu *et al.*, « End-of-life or second-life options for retired electric vehicle batteries », *Cell Reports Physical Science*,
 489 vol. 2, n° 8, p. 100537, août 2021, doi: [10.1016/j.xcrp.2021.100537](https://doi.org/10.1016/j.xcrp.2021.100537).
- 490 [41] Y. Miao, P. Hynan, A. von Jouanne, et A. Yokochi, « Current Li-Ion Battery Technologies in Electric Vehicles and
 491 Opportunities for Advancements », *Energies*, vol. 12, n° 6, Art. n° 6, janv. 2019, doi: [10.3390/en12061074](https://doi.org/10.3390/en12061074).
- 492 [42] C. Chan, A. Bouscayrol, K. Chen, "Electric, Hybrid and Fuel Cell Vehicles: Architectures and Modeling", *IEEE*
 493 *Transactions on Vehicular Technology*, vol. 59, no. 2, pp. 589-598, February 2010
- 494 [43] H. Wang, Y. Huang, H. He, W. Liu, A. Khajepour, "Energy Management of hybrid, electric vehicle", *Modelling,*
 495 *dynamics and control of electrified vehicles*, Chapter 5, Elsevier, 2018.
- 496